This is an Accepted Manuscript version of the following article, accepted for publication in:

Analytical Model to Calculate Radial Forces in Permanent-Magnet Synchronous Machines

Iratxo Gómez[1], Gaizka Almandoz[1], *Member, IEEE*, Javier Poza[1], *Member, IEEE*,
Gaizka Ugalde[1], *Member, IEEE,* Ana Julia Escalada[2]

[1] University of Mondragon, 20500 Arrasate – Mondragon
[2] ORONA Elevator Innovation Centre, 20120 Hernani

Abstract—In permanent-magnet synchronous machines (PMSMs) electromagnetic forces are identified as the principal source of vibrations and noises. In this article, first of all the sources of magnetic forces in PMSMs are analyzed. Then, an analytical method for the calculation of radial forces on the base of the stator tooth created by electromagnetic sources in PMSMs is presented. Finally finite element method (FEM) is used to corroborate analytical results.

Index Terms—Finite element method, Fourier spatial series, Maxwell stress tensor, Noise and vibration, Permanent-magnet synchronous machine.

I. INTRODUCTION

NOWADAYS, electric machines are considered a mature technology. A good indicator is that in developed cities more than 65% of the electrical consumption is made by electric machines [1]. However, the necessity of improving products due to the increase in competitiveness and in quality standards has pushed forward the study of aspects like vibrations and noises [2]. These issues take special importance if the application environment is near of human life, such as home appliances, medical instruments, elevators, electric vehicles and so on [3].

The noises and vibrations generated by an electric motor have different sources that can be classified in three families [1], [2], [4]:

- Electromagnetic source.
- Mechanical source.
- Aerodynamic source.

In PMSMs without severe working conditions the fan can be eliminated and the noises and vibrations generated by bearings and shaft misalignment can be reduced considerably in the manufacture process. Hence, as can be seen in Fig.1 and is stated in [2–5] the electromagnetic source is the dominating one.

In electric machines that do not use the reluctance principle the electromechanical energy conversion is due to an interaction between two magnetic fields in the air gap [4]. In PMSMs the stator field is created by coils and the rotor field is produced by permanent magnets which are located in the rotor, hence the name. From the analysis of these fields plenty of characteristic of the machine, electromagnetic torque, electromagnetic forces (EMF), et cetera [6–9] can be obtained.

I. Gómez, G. Almandoz, J. Poza, and G. Ugalde are with the University of Mondragón, 20500 Arrasate – Mondragón.

A.J. Escalada is with ORONA Elevator Innovation Centre, 20120 Hernani. (e-mail: igomezs@mondragon.edu; galmandoz@mondragon.edu; jpoza@mondragon.edu; gugalde@mondragon.edu; ajescalada@orona-group.com).
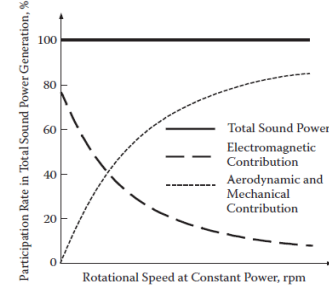
Fig.1. Contribution of different sources to sound power radiation [1].

Numerous designers use FEM to obtain this information. The principal drawbacks of FEM are computational costs and therefore design times. To minimize these problems some researchers try to analyse the machine without FEM. One possible approximation of the magnetic fields is to assume a rectangular distribution. Few authors base their work in this method because the distribution is not really completely rectangular. Some researchers use trapezoidal approximations for direct current (DC) motors [10]. Other ones propose empirical approximations [11], [12]. Zhu is one of the researchers with more publications about the modelling of PMSMs based on Fourier spatial series. In [13–16] Zhu creates a complete model of a DC machine. The method is based on Fourier spatial series resolved in polar coordinates. At present it is possible to find other authors who use similar models [17]. There are different studies about magnetic forces in which the calculi are based on the application of Maxwell tensor's law in the magnetic flux densities [18–21]. In these researches the influence of the permeance, slot/pole combinations, acoustic models or the unbalance of the system are analysed.

In this article the Fourier spatial series are resolved in Cartesian coordinates and equations of the analytical model are fully developed in relation to the physical parameters of the machine. These are the reasons why the traceability of the problematic harmonics to eliminate or reduce them is easier and quicker. The tool is based on [22–24] and thanks to it a mathematical model of the machine in steady state which is used to analyse motor performance parameters such as magnetic fields, radial forces and so on is obtained. The model is validated in two different machines as can be seen in Table I and section *IV*.

TABLE I
PRINCIPAL CHARACTERISTICS OF SIMULATED MACHINES.

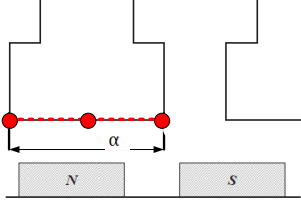| Machine	Slots number	Pair poles number	Layers number
Qs48p8	48	8	1
Qs36p15	36	15	2

Fig.2. Periphery of stator where the magnetic pressures are analysed.

II. SOURCES OF MAGNETIC FORCES IN PMSMS

As it is well known the functioning principle of a PMSM is based on the interaction of two magnetic fields in the air gap. These magnetic fields generate magnetic pressures and forces around stator´s and rotor's surfaces that are in contact with the air-gap. The magnetic forces generated in PMSMs can be caused by three different sources: magnetic pressures originated in the stator, magnetic pressures originated in the rotor and forces created by eccentricities. In this section all these sources are analyzed.

A. Magnetic Pressures in the Stator

The flux density in the periphery of the stator is formed by radial and tangential components. These components generate a magnetic radial pressure that can be calculated applying the Maxwell tensor's law.

$$P_r(t,\theta) = \frac{1}{2\mu_0}\left[\left(B_{sr}^m(t,\theta)\right)^2 - \left(B_{st}^m(t,\theta)\right)^2\right]\left[\frac{N}{m^2}\right] \quad (1)$$

Where μ_0 is the permeability of the vacuum, and $B_{sr}^m(t,\theta)$ and $B_{st}^m(t,\theta)$ are the radial and the tangential components respectively of the flux density around the periphery of stator's tooth.

The radial component of the flux density is much bigger than tangential component so it can be neglected to obtain the next simplified equation.

$$P_r(t) = \frac{1}{2\mu_0}\left(B_{sr}^m(t,\theta)\right)^2\left[\frac{N}{m^2}\right] \quad (2)$$

The radial component of the magnetic flux density in the periphery of the stator can be defined by Fourier spatial series with (3).

$$B_{sr}^m(t,\theta) = \sum_{n=-\infty}^{+\infty} B_{sn}^m \cos\left(pn(\varphi + \Omega_m t - \theta)\right) \text{ [T]} \quad (3)$$

B_{sn}^m are coefficients of Fourier series, p is the number of pole pairs, n is the harmonic's order, φ is the magnet's initial position, Ω_m is the mechanical speed, t is the time and θ is the position around the tooth.

Replacing (3) in (2) the next equation can be obtained.

$$P_r(t,\theta) = \frac{1}{2\mu_0}\left[\sum_{n=-\infty}^{+\infty} B_{sn}^m \cos\left(pn(\Omega_m t - \theta)\right) \right.$$
$$\left. \cdot \sum_{n=-\infty}^{+\infty} B_{sk}^m \cos\left(pk(\Omega_m t - \theta)\right)\right]\left[\frac{N}{m^2}\right] \quad (4)$$

Using the well-known trigonometric property $cos(\alpha)\cos(\beta) = \frac{1}{2}cos(\alpha \pm \beta)$ the following expression for the magnetic pressure is deduced.

$$P_r(t,\theta) = \sum_{n=1}^{+\infty}\sum_{k=1}^{+\infty} \frac{B_{sn}^m B_{sk}^m}{4\mu_0} \cdot cos\left(\pm(n \pm k)p(\Omega_m t + \theta)\right)\left[\frac{N}{m^2}\right] \quad (5)$$

TABLE II
RELATIONSHIP BETWEEN HARMONICS OF THE FLUX DENSITY AND HARMONICS OF THE MAGNETIC PRESSURE IN THE STATOR.

Flux density harmonics		Magnetic pressure harmonics	Flux density harmonics		Magnetic pressure harmonics
n	k	μ=±(n±k)	n	k	μ=±(n±k)
±1	±1	0 / ±2	±5	±1	±4 / ±6
	±3	±2 / ±4		±3	±2 / ±8
	±5	±4 / ±6		±5	0 / ±10
	±7	±6 / ±8		±7	±2 / ±12
	±9	±8 / ±10		±9	±4 / ±14
±3	±1	±2 / ±4	±7	±1	±6 / ±8
	±3	0 / ±6		±3	±4 / ±10
	±5	±2 / ±8		±5	±2 / ±12
	±7	±4 / ±10		±7	0 / ±14
	±9	±6 / ±12		±9	±2 / ±16

From (5) the Table II is deduced. In that table the relationship between the harmonics of the flux density and the harmonics of the magnetic pressure is represented.

It is important to note that all harmonics of the magnetic pressure are even for any combination of pole pairs and stator slots. In the same way, all harmonics of the flux density are odd. Other interesting aspect of the Table II is that provides information about the flux density harmonics that must be eliminated to reduce a component of the magnetic pressure. The magnet pitch can be modified to eliminate these flux density harmonics, (17).

B. Magnetic Pressures in the Rotor

The oscillating magnetic pressure on the rotor surface is due to a variation in the flux density that crosses the rotor surface. This variation can be caused by the stator slots and by the magnetic flux density created by the armature.

1) Oscillating Magnetic Pressure Due to Slots

In a slotless machine the air-gap reluctance seen by the rotor is constant. In this case, if the machine works in open circuit mode the flux density in the air-gap is created only by the magnets and therefore flux density crossing the rotor surface is constant. Otherwise, the flux density crossing the stator surface is not constant; it varies at the electrical frequency. As it is well known, that frequency is the mechanical one multiplied by the number of pair poles.

Focusing on the rotor, as aforementioned, in a slotless machine the magnetic flux crossing the rotor surface is constant so that the magnetic pressure on the same surface is also constant. However in case of a slotted stator, the air-gap reluctance is not constant what leads to a variation in the flux density crossing the rotor surface. The frequency of that variation references to the stator currents depends on the number of slots and poles, and it can be defined by (6).

$$n = k\frac{Q_s}{p}, \quad k \in \mathbb{N} \quad (6)$$

Q_s is the number of slots. To calculate the magnetic pressures on the rotor surface, the simplified equation of the Maxwell's tensor law (2) can be used. In Table III the relationship between flux density and magnetic pressure harmonics is shown. In this case the harmonics cannot be eliminated like in the stator. However modifying the Q_s/p relation they can be displaced from problematic frequencies.

TABLE III
RELATIONSHIP BETWEEN HARMONICS OF THE FLUX DENSITY AND HARMONICS OF THE MAGNETIC PRESSURE IN THE ROTOR.

Flux density harmonics		Magnetic pressure harmonics	Flux density harmonics		Magnetic pressure harmonics
n	k	μ=±(n±k)	n	k	μ=±(n±k)
±Q$_s$/p	±Q$_s$/p	0 / ±2Q$_s$/p	±3Q$_s$/p	±Q$_s$/p	±2Q$_s$/p / ±4Q$_s$/p
	±2Q$_s$/p	±Q$_s$/p / ±3Q$_s$/p		±2Q$_s$/p	±Q$_s$/p / ±5Q$_s$/p
	±3Q$_s$/p	±2Q$_s$/p / ±4Q$_s$/p		±3Q$_s$/p	0 / ±6Q$_s$/p
	±4Q$_s$/p	±3Q$_s$/p / ±5Q$_s$/p		±4Q$_s$/p	±Q$_s$/p / ±7Q$_s$/p
	±5Q$_s$/p	±4Q$_s$/p / ±6Q$_s$/p		±5Q$_s$/p	±2Q$_s$/p / ±8Q$_s$/p
±2Q$_s$/p	±Q$_s$/p	±Q$_s$/p / ±3Q$_s$/p	±4Q$_s$/p	±Q$_s$/p	±3Q$_s$/p / ±5Q$_s$/p
	±2Q$_s$/p	0 / ±4Q$_s$/p		±2Q$_s$/p	±2Q$_s$/p / ±6Q$_s$/p
	±3Q$_s$/p	±Q$_s$/p / ±5Q$_s$/p		±3Q$_s$/p	±Q$_s$/p / ±7Q$_s$/p
	±4Q$_s$/p	±2Q$_s$/p / ±6Q$_s$/p		±4Q$_s$/p	0 / ±8Q$_s$/p
	±5Q$_s$/p	±3Q$_s$/p / ±7Q$_s$/p		±5Q$_s$/p	±Q$_s$/p / ±9Q$_s$/p

2) Magnetic Pressure Created by the Stator Armature

The principal component of the flux density created by the armature propagates along the air gap in synchronism with the main component of the flux density created by the magnets. In other words, it propagates in the same direction and with the same mechanical speed of the rotor, Ω_m. However, the other spatial components propagate asynchronously with the rotor at the Ω_n velocity.

$$\Omega_m = \frac{w_s}{p} \left[\frac{\text{rad}}{\text{s}}\right] \qquad \Omega_n = \frac{w_s}{s \cdot n \cdot t_p} \left[\frac{\text{rad}}{\text{s}}\right] \tag{7}$$

w_s is the electrical speed of the rotor, t_p is the periodicity as the greatest common divisor between Q_s and p, and $s = \pm 1$ defines the direction of the propagation.

The pulsation of a component of the armature flux density referenced to the rotor, Ω_{rn}, is the subtraction between the rotor speed, Ω_m, and the propagation velocity of the component, Ω_n.

$$\Omega_{rn} = \Omega_n - \Omega_m = \left(\frac{p}{s \cdot n \cdot t_p} - 1\right)\Omega_m \left[\frac{\text{rad}}{\text{s}}\right] \tag{8}$$

Therefore, the frequency of this component referenced to the rotor, f_{rn}, is defined as:

$$f_{rn} = \frac{n \cdot t_p \cdot \Omega_{rn}}{2\pi} = \left(s\frac{p}{t_p} - n\right)\frac{t_p}{p}f_s \text{ [H}_z] \tag{9}$$

f_s represents the supplying frequency. Therefore, the harmonics order of the magnetic flux density can be calculated as:

$$k = \left(s\frac{p}{t_p} - n\right)\frac{t_p}{p} \tag{10}$$

Analysing the previous equation it can be deduced that the harmonics order of the armature flux density referenced to the rotor, depends on p/t_p. Hence, it can be said that they are related with the slots and the pole pairs.

Once identified the harmonics of the armature flux density referenced to the rotor, using the Maxwell's tensor law (2), it is possible to identify the harmonics of the magnetic pressure on the rotor.

TABLE IV
FLUX DENSITY HARMONICS CREATED BY THE ARMATURE REFERENCE TO THE STATOR AND TO THE ROTOR IN QS48P8 MACHINE.

Fixed reference (Stator)		Moving reference (Rotor)
Order	Sign	Order
n=1	s=1	(s-n)=0
n=5	s=-1	(s-n)=-6
n=7	s=1	(s-n)=-6
n=11	s=-1	(s-n)=-12
n=13	s=1	(s-n)=-12

TABLE V
FLUX DENSITY HARMONICS CREATED BY THE ARMATURE REFERENCE TO THE STATOR AND TO THE ROTOR IN QS36P15 MACHINE.

Fixed reference (Stator)		Moving reference (Rotor)
Order	Sign	Order
n=1	s=-1	(5s-n)/5=-1.2
n=5	s=1	(5s-n)/5=0
n=7	s=-1	(5s-n)/5=-2.4
n=11	s=1	(5s-n)/5=-1.2
n=13	s=-1	(5s-n)/5=-3.6

TABLE VI
RELATIONSHIP BETWEEN HARMONICS OF THE FLUX DENSITY AND HARMONICS OF THE MAGNETIC PRESSURE IN THE ROTOR CREATED BY THE ARMATURE IN A QS48P8 MACHINE

Flux density harmonics		Magnetic pressure harmonics	Flux density harmonics		Magnetic pressure harmonics
n	k	μ=±(n±k)	n	k	μ=±(n±k)
0	0	0	-12	0	±12
	-6	±6		-6	±18/±6
	-12	±12		-12	±24/0
	-18	±18		-18	±30/±6
-6	0	-±6	-18	0	±18
	-6	±12/0		-6	±24/±12
	-12	±18/±6		-12	±30/±6
	-18	±24/±12		-28	±46/±10

TABLE VII
RELATIONSHIP BETWEEN HARMONICS OF THE FLUX DENSITY AND HARMONICS OF THE MAGNETIC PRESSURE IN THE ROTOR CREATED BY THE ARMATURE IN A QS36P15 MACHINE

Flux density harmonics		Magnetic pressure harmonics	Flux density harmonics		Magnetic pressure harmonics
n	k	μ=±(n±k)	n	k	μ=±(n±k)
0	0	0	-2.4	0	±2.4
	-1.2	±1.2		-1.2	±1.2/±3.6
	-2.4	±2.4		-2.4	±4.8/0
	-3.6	±3.6		-3.6	±1.2/±6
	-4.8	±4.8		-4.8	±7.2/±2.4
-1.2	0	±1.2	-3.6	0	±3.6
	-1.2	±2.4/0		-1.2	±4.8/±2.4
	-2.4	±1.2/±3.6		-2.4	±1.2/±6
	-3.6	±4.8/±2.4		-3.6	±7.2/0
	-4.8	±3.6/±6		-4.8	±1.2/±8.4

C. Magnetic Forces due to Eccentricities

Eccentricities in electrical machines can be classified as static, dynamic and mixed eccentricities. It is known as static eccentricity when the rotating shaft of the rotor is the centre of the rotor and it is not aligned with the centre of the stator. Dynamic eccentricity occurs when the rotating shaft of the rotor is not aligned with its own centre, but it is aligned with the stator's centre. Finally, mixed eccentricity appears when the previously described two cases are combined. In this case, the rotating shaft of the rotor is not aligned with either the rotor's centre or stator's centre. These eccentricities can be seen in the Fig.3.

The effect of the eccentricity can be taken into account multiplying the magnetic flux density of the air-gap by a distribution function, Δ_ϵ. This function describes the variation of the air-gap reluctance due to the eccentricity.

a) Static   b) Dynamic   c) Mixed
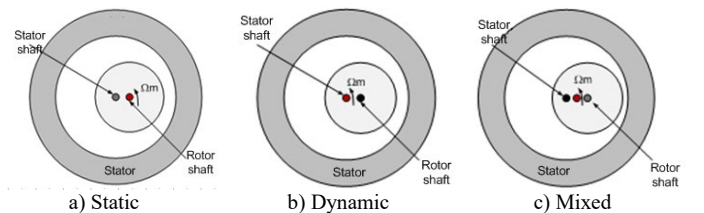
Fig.3. Types of eccentricity. The Red shaft represents the rotation axis.

$$B_{g\epsilon}(t,\theta) = B_g(t,\theta) \cdot \Delta_\epsilon(t,\theta) \ [T] \tag{11}$$

The variation of the air-gap can be represented by (12). In order to simplify the analysis only the main components of Δ_ϵ and B_g functions are considered.

$$\Delta_\epsilon(t,\theta) = \Delta_{\epsilon 1} cos\,(\theta - \Omega_m t) \tag{12}$$

Finally, substituting only the fundamental component of flux density in (3) and multiplying by (12) the flux density in the air-gap can be expressed considering the eccentricity.

$$B_{g\epsilon}(t,\theta) = B_{g1}\,cos(p\theta + p\Omega_m t) \\ \cdot \Delta_{\epsilon 1}\,cos(\theta - \Omega_m t)\ [T] \tag{13}$$

Using the trigonometric property $cos(\alpha)\,cos(\beta) = \frac{1}{2}cos(\alpha \pm \beta)$ and developing (13) the following expression is obtained.

$$B_{g\epsilon}(t,\theta) = \frac{1}{2}B_{g1}\Delta_{\epsilon 1}\,cos(\nu_\epsilon \cdot p \cdot \theta \pm (w_s \pm \Omega_m)t)\ [T] \tag{14}$$

In case of static eccentricities, $\Omega_m = 0\,\frac{rad}{s}$. Due to eccentricities new harmonics appear in the flux density on the air-gap. The order of this new harmonics can be obtained by (15).

$$\nu_\epsilon = 1 \pm \frac{1}{p} \tag{15}$$

III. ANALYTICAL MODEL

The proposed analytical model was developed in four steps. In the first two steps the computation of the flux density created by magnets and coils in a slotless machine is addressed. Then the slots effect is obtained and added to the flux densities. Finally the two flux densities are superimposed in order to obtain the overall flux density in load conditions.

A. Magnetic Flux Density Created by Magnets in a Slotless Machine

In PMSMs with a rotor of non-consecutive poles, the magnitude of the flux density created by the magnets in the air-gap can be calculated as it is shown in (16).

$$\hat{B}_g = \frac{B_r}{1 + \frac{g\mu_{rm}}{h_m}}\ [T] \tag{16}$$

Where B_r is the remanent value of the magnets field, h_m is the height of the magnets, g is the length of the air-gap and μ_{rm} is the relative permeance of the magnets.

Once the magnitude is calculated, next the spatial distribution of this flux density can be represented by Fourier series (3). Coefficients of the series are calculated by the next expression.

$$B_{gn}^m = \frac{\hat{B}_g}{n\pi}(1 - cos(n\pi))\,sin\left(n \cdot p\,\frac{\beta_m}{2}\right)\frac{2}{1 + (a \cdot n \cdot p)^2} \tag{17}$$

β_m is the magnet pitch, and a is a parameter known as fringing coefficient. This fringing coefficient is used to avoid a rectangular distribution with the aim of obtaining more accurate results, as can be seen in Fig.4. It can be parameterized as a function of different dimensions of the machine in order to find a physical meaning [11], [23], [25].
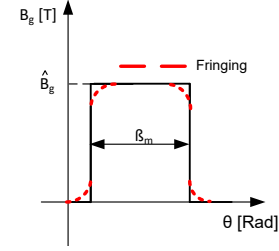

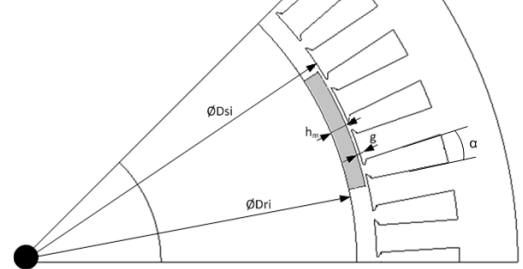Fig.4. Spatial distribution of the field with a and without a.

Fig.5. Principal dimensions of the machine.

$$a = \frac{\sqrt{g\left(g + \frac{h_m}{\mu_{rm}}\right)}}{D_{ri} + 2h_m + g} \tag{18}$$

Where D_{ri} is the inner diameter of the rotor.

B. Magnetic Flux Density Created by Coils in a Slotless Machine

Magnetic flux density created by coils in the air-gap is calculated by the next expression.

$$B_g^a(t,\theta) = \mu_0 \cdot \frac{F_{MM}(t,\theta)}{g}\ [T] \tag{19}$$

F_{MM} is the magneto motive force created by the coils in the air-gap. To obtain the F_{MM}, conductors distribution must be known. This distribution is defined as the variation of the magneto motive force per unit of current in the air-gap and is defined by the start of slots tool. There are different ways to use this tool. In [26] a double layer start of slots is done and then if the machine requires and if it is possible it is modified to a single layer. In this article the used procedure follows [24] as can be seen in Fig. 6.

Once the physical distribution of the conductors is known, first the winding factor, Kw_n, can be calculated applying (20), and then the magneto motive force per current unit can be computed by (21).

$$Kw_n = \frac{\sum_{k=0}^{k=h-1} e^{j \cdot n \cdot t_p \cdot (\varphi_k)} - e^{j \cdot n \cdot t_p \cdot (\varphi_k + \varphi)}}{\sum_{k=0}^{k=h-1}\left|e^{j \cdot n \cdot t_p \cdot (\varphi_k)} - e^{j \cdot n \cdot t_p \cdot (\varphi_k + \varphi)}\right|} = \\ = \xi_n \cdot e^{j \cdot n \cdot t_p \cdot \varphi_{ph}} \tag{20}$$
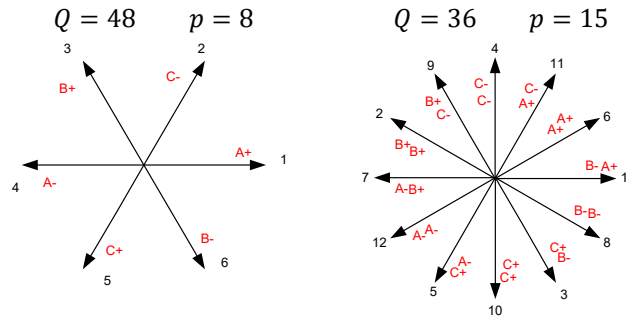

Fig. 6. Star of slots.

$$F_{an} = \frac{-j2hN}{\pi n^2 \alpha t_p} sin\left(\frac{n \cdot t_p \cdot \alpha}{2}\right)\xi_n e^{j\cdot n \cdot t_p \cdot \varphi_{ph}}$$

$$F_a(\theta) = \sum_{n=-\infty}^{n=+\infty} F_{an} e^{j\cdot n \cdot t_p \cdot (\varphi_{ph}-\theta)} \tag{21}$$

h is the number of coils per phase, φ_k the position angle of each coil, φ the coil pitch angle, N the number of turns and α the angle in which the conductors are distributed, Fig.5. Then the F_a is multiplied by the current of its phase (22) and finally the magneto motive force of all phases are summed (23).

$$F_{MMa}(t,\theta) = F_a(\theta) \cdot i_A(t) \tag{22}$$

$$F_{MM}(t,\theta) = F_{MMa}(t,\theta) + F_{MMb}(t,\theta) + F_{MMc}(t,\theta) \tag{23}$$

Finally (19) is applied. It is important to note that the phase difference between magneto motive forces of different phases is the same that is between currents, $\frac{2\pi}{3}$ radians. That is the reason why (24) can be deduced from (23).

$$F_{MM}(t,\theta) = \sum_{n=-\infty}^{n=+\infty} F_{an} e^{-jnt_p\theta} i e^{jW_e t}$$
$$\cdot \left[1 + 2\cos\left(\frac{2\pi}{3}(n-1)\right)\right] \tag{24}$$

It can be seen from (24) that some harmonics of the F_{MM} are cancelled when the magneto motive force of all phases are summed.

C. Effect of Stator Slots

Previously cited expressions are oriented to a slotless machine. In a machine with slots the permeance variation is must be known. This effect is analyzed in [15], where a conformal transformation is proposed from Z plane to W plane to obtain the permeance of the Fig.7.

When the permeance variation of a slot is obtained, Fig.7, the variation for all the machine can be reconstructed with (25).

$$\lambda(\theta) = \lambda_0 + \sum_{n=1}^{+\infty} \lambda_n \cos\left(Q_s n(\Theta - \theta)\right) \tag{25}$$

Where λ_0 is the mean value of the variation of the permeance, λ_n is the 'n' order Fourier coefficient and Θ is the initial position of the slot. Finally to represent the flux density in slotted machines, (25) and the flux density must be multiplied. For the magnet case (17) and (25) are multiplied, Fig.8.

$$B_{g\,slot}^a(t,\theta) = B_g^a(t,\theta)\lambda(\theta) \quad [T] \tag{26}$$

D. Magnetic Forces in the Stator

The magnetic radial pressure is calculated with the Maxwell tensor's law as can be seen in section *II.A.* using (2). Finally to obtain the magnetic radial force on the base of the stator tooth (27) is used.
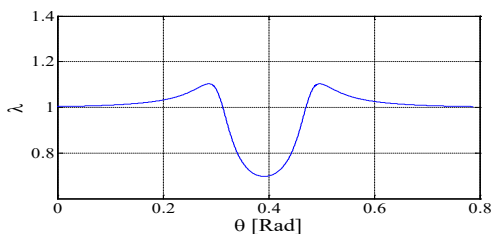

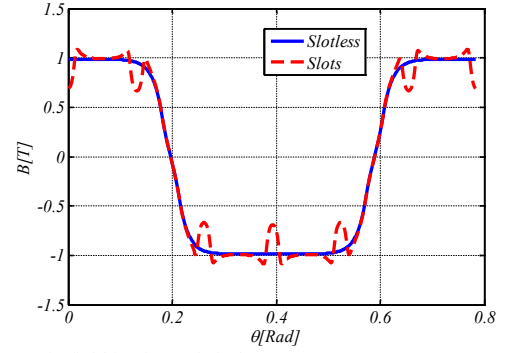Fig.7. Variation of the radial permeance due to the effect of a slot.

Fig.8. Magnetic field in slot and slotless stator.

$$F_r(t) = \frac{L_e \cdot D_{si}}{2} \int_0^\alpha P_r(t,\theta)\,d\theta \quad [N] \tag{27}$$

L_e is the length of the machine and D_{si} is the interior diameter of the stator, Fig.5.

IV. VALIDATION

A. Introduction

The results of the analytical model are corroborated with a FEM software, specifically Flux CEDRAT. In this software two paths are defined: one in the middle of the air-gap and other one in the base of the tooth, Fig.2. With the first path the flux densities are obtained and with the second magnetic pressures and also flux densities. Finally the magnetic forces are calculated with (27).

The comparison of the methods is realized using two different machines. The principal characteristics of these machines are summarised in Table I. The main differences between them are the number of pair poles, the number of slots and the number of winding layers.

B. Results

In the next illustrations the results of the analytical or Fourier model versus results of the FEM program are shown.

1) Magnetic Field

As can be seen in Fig.9 and in Fig.10 the results of the analytical tool in the magnetic flux densities are quite accurate.
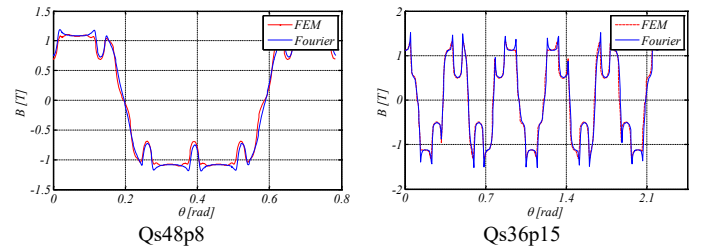

Qs48p8   Qs36p15
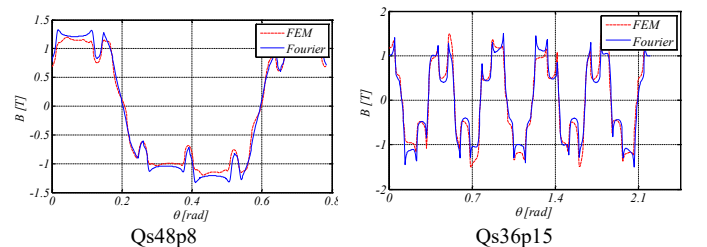Fig.9. Flux density created by magnets in open circuit operation.

Qs48p8   Qs36p15
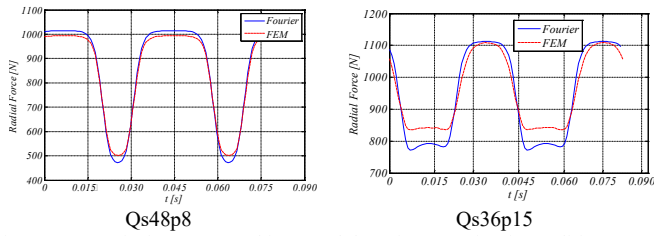Fig.10. Flux densities created by magnets and coils in load operation.

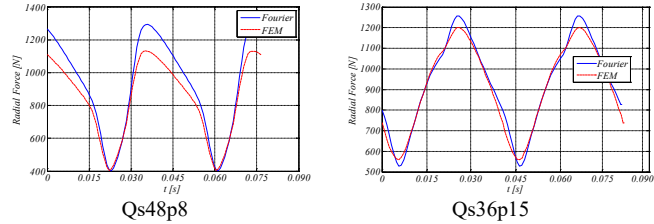Fig.11. Magnetic forces created in a tooth base in open circuit condition.

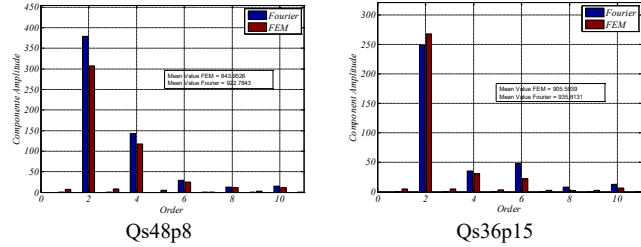Fig.12. Magnetic forces created in a tooth base in load condition.

Fig.13. Harmonics of magnetic forces created in a tooth in load condition.

2) Magnetic Forces

Magnetic forces created by magnets in open circuit, Fig.11, and in load condition, Fig.12, are also good, as well as the orders of the components, Fig.13.

3) Magnetic Pressure

The difference of the magnetic forces comes from the difference in the calculus of the magnetic pressures in the edges of the tooth. If the magnetic pressures are examined, Fig.14 and Fig.15, in the middle of the tooth, it can be seen how the results agree but this not occur in the edges of the tooth. The reason of this discrepancy is the difference of the magnetic flux densities in the edges of the tooth, Fig.16. and Fig.17. That is why the results in the middle of the slot have better accuracy than in the edge of slots.
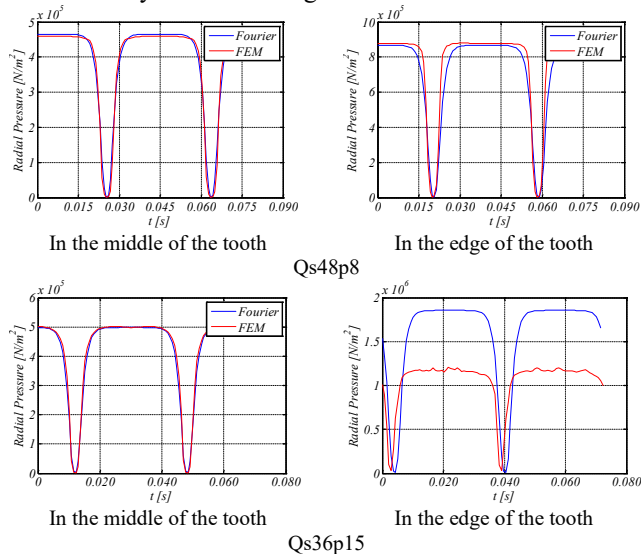

In the middle of the tooth | In the edge of the tooth
Qs48p8

In the middle of the tooth | In the edge of the tooth
Qs36p15

Fig.14. Magnetic pressures created by magnets in open circuit operation.

In the middle of the tooth | In the edge of the tooth
Qs48p8

In the middle of the tooth | In the edge of the tooth
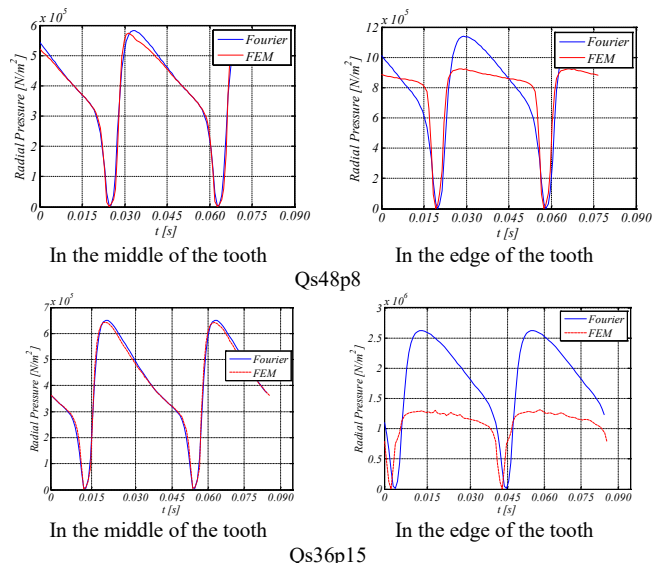Qs36p15

Fig.15. Magnetic pressures created by magnets and coils in load operation.
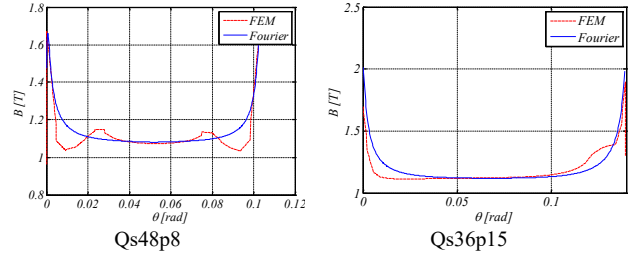

Qs48p8 | Qs36p15

Fig.16. Flux density difference in the tooth base in open circuit operation.
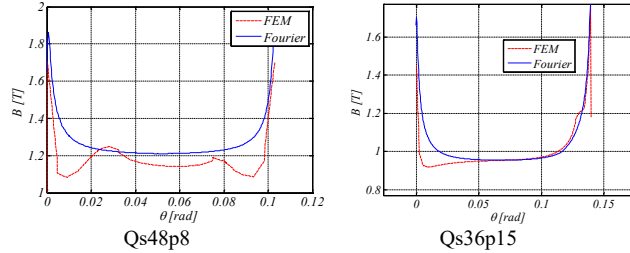

Qs48p8 | Qs36p15

Fig.17. Flux density difference in a tooth base in load condition.

V. CONCLUSIONS

This article presents an analytical model based on spatial Fourier series to represent the flux density created in a machine in open circuit and load operation conditions. Then radial magnetic forces and pressures created by these flux densities are analysed by the model.

Two machines are studied with FEM, concretely with Flux CEDRAT, to corroborate the results of the analytical model. The model shows a good agreement with the FEM results especially in the identification of the harmonics.

The main advantages of the model compared to the FEM method are the rapidity of the calculi and the easiness to relate components of the flux density and magnetic forces to design variables. So using the proposed model an iterative optimization of the machine design may be performed in a relatively easy and quick way.

Future work will be needed to include into the model eccentricities and magnetic pressures in the rotor.

VI. References

[1] C. Taylor, F. Group, and M. O. Thurston, *Noise of Polyphase Electric Motors*. 2006.

[2] A. Mccloskey Gómez, "Predicción del Comportamiento Vibratorio y Acústico de una Máquina Eléctrica." Mondragon Goi Eskola Politeknikoa, pp. 1–92, 2013.

[3] T. Sun, J.-M. Kim, G.-H. Lee, J.-P. Hong, and M.-R. Choi, "Effect of Pole and Slot Combination on Noise and Vibration in Permanent Magnet Synchronous Motor," *IEEE Transactions on Magnetics*, vol. 47, no. 5, pp. 1038–1041, May 2011.

[4] R. Islam and I. Husain, "Analytical Model for Predicting Noise and Vibration in Permanent-Magnet Synchronous Motors," *IEEE Transactions on Industry Applications*, vol. 46, no. 6, pp. 2346–2354, Nov. 2010.

[5] G. He, Z. Huang, R. Qin, and D. Chen, "Numerical Prediction of Electromagnetic Vibration and Noise of Permanent-Magnet Direct Current Commutator Motors With Rotor Eccentricities and Glue Effects," *IEEE Transactions on Magnetics*, vol. 48, no. 5, pp. 1924–1931, May 2012.

[6] H. C. M. Mai, R. Bernard, P. Bigot, F. Dubas, D. Chamagne, and C. Espanet, "Consideration of Radial Magnetic Forces in Brushless DC Motors." Incheon, pp. 1–6, 2010.

[7] D. Cho and K. Kim, "Modelling of Electromagnetic Excitation Forces of Small Induction Motor for Vibration and Noise Analysis," *Electric Power Applications, IEEE Proceedings*, vol. 145, no. 3, pp. 199–205, 1998.

[8] S. P. Verma and A. Balan, "Experimental Investigations on the Stators of Electrical Machines in Relation to Vibration and Noise Problems," *Electric Power Applications, IEEE Proceedings*, vol. 145, no. 5. IET, 1998.

[9] S. P. Verma, "Noise and Vibrations of Electrical Machines and Drives; their Production and Means of Reduction," *Proceedings of the 1996 international conference on power electronics, drives and energy systems for industrial growth, New Delhi*, vol. 2, pp. 1031–1037, 1996.

[10] B. Ackermann, R. Sottek, J. H. H. Janssen, and R. I. van Steen, "New Technique for Reducing Cogging Torque in a Class of Brushless DC Motors," *Electric Power Applications, IEEE Proceedings*, vol. B 139, no. 4, pp. 315–320, 1992.

[11] T. J. E. Miller and R. Rabinovici, "Back-EMF Waveforms and Core Losses in Brushless DC Motors," *IEEE Proceedings on Electric Power Applications Proceedings on Electric Power Applications*, vol. 141, no. 3, pp. 144–154, 1994.

[12] Tomy Sebastian and Vineeta Gangla, "Analysis of Induced EMF Waveforms and Torque Ripple in a Brushless Permanent Magnet Machine," *IEEE Transactions on Industry Applications*, vol. 32, no. 1, pp. 195–200, 1996.

[13] Z. Q. Zhu, D. Howe, E. Bolte, and B. Ackerman, "Instantaneous Magnetic Field Distribution in Brushless Permanent Magnet DC Motors. I. Open-circuit field," *IEEE Transactions on Magnetics*, vol. 29, no. 1, pp. 124–135, 1993.

[14] Z. Q. Zhu and D. Howe, "Instantaneous Magnetic Field Distribution in Brushless Permanent Magnet DC Motors. II. Armature-Reaction Field," *IEEE Transactions on Magnetics*, vol. 29, no. 1, pp. 136–146, 1993.

[15] Z. Q. Zhu and D. Howe, "Instantaneous Magnetic Field Distribution in Brushless Permanent Magnet DC Motors. III. Effect of Stator Slotting," *IEEE Transactions on Magnetics*, vol. 29, no. 1, pp. 143–151, 1993.

[16] Z. Q. Zhu and D. Howe, "Instantaneous Magnetic Field Distribution in Permanent Magnet Brushless DC Motors, Part IV: Magnetic Field on Load," *IEEE Transactions on Magnetics*, vol. 29, no. 1, pp. 152–158, 1993.

[17] A. B. Proca, A. Keyhani, A. EL-Antably, W. Lu, and D. M., "Analytical Model for Permanent Magnet Motors with Surface Mounted Magnets," *IEEE Transactions on Energy Conversion*, vol. 18, no. 3, pp. 386–391, 2003.

[18] D. Verdyck and R. J. M. Belmans, "An Acoustic Model for a Permanent Magnet Machine: Modal Shapes and Magnetic Forces," *IEEE Transactions on Industry Applications*, vol. 30, no. 6, p. 1625, Nov. 1994.

[19] Z. Zhu, D. Ishak, D. Howe, and J. Chen, "Unbalanced magnetic forces in permanent-magnet brushless machines with diametrically asymmetric phase windings," *Industry Applications, IEEE Transactions*, vol. 43, no. 6, pp. 1544–1553, 2007.

[20] L. J. Wu, Z. Q. Zhu, J. T. Chen, and Z. P. Xia, "An Analytical Model of Unbalanced Magnetic Force in Fractional-Slot Surface-Mounted Permanent Magnet Machines," *IEEE Transactions on Magnetics*, vol. 46, no. 7, pp. 2686–2700, Jul. 2010.

[21] G. Dajaku and D. Gerling, "The Influence of Permeance Effect on the Magnetic Radial Forces of Permanent Magnet Synchronous Machines," *IEEE Transactions on Magnetics*, vol. 49, no. 6, pp. 2953–2966, Jun. 2013.

[22] G. Almandoz, J. Poza, M. A. Rodriguez, and A. Gonzalez, "Analytic model of a PMSM considering spatial harmonics," *Power Electronics, Electrical Drives, Automation and Motion, 2008. SPEEDAM 2008. International Symposium on*, pp. 603–608, 2008.

[23] A. Egea, G. Almandoz, J. Poza, and A. Gonzalez, "Analytic model of axial flux permanent magnet machines considering spatial harmonics," *Power Electronics Electrical Drives Automation and Motion (SPEEDAM), 2010 International Symposium on*, pp. 495–500, 2010.

[24] G. Ugalde, J. Poza, M. A. Rodriguez, and A. Gonzalez, "Space harmonic modeling of fractional permanent magnet machines from star of slots," *Electrical Machines, 2008. ICEM 2008. 18th International Conference on*, pp. 1–6, 2008.

[25] J. R. Hendershot and T. J. E. Miller, *Design of Brushless Permanent-Magnet Machines*. Motor Desing Books, 2010.

[26] N. Bianchi and M. Dai Pré, "Use of the Star of Slots in Designing Fractional-Slot Single-Layer Synchronous Motors," *Electric Power Applications, IEEE Proceedings*, vol. 153, no. 3, pp. 459–466, 2006.

VII. Biographies

Iratxo Gómez was born in Vitoria, Spain, in June 1989. He received the B.S. degree in electrical engineering from the University of Mondragón, Mondragón, Spain, in 2013, where he is currently working toward the Ph.D. degree. His current research interests include permanent magnet machine design and optimization.

Gaizka Almandoz was born in Arantza, Spain, in March 1979. He received the B.S. and Ph.D. degrees in electrical engineering from the University of Mondragón, Mondragón, Spain, in 2003 and 2008, respectively. Since 2003, he has been with the Department of Electronics, Faculty of Engineering, University of Mondragón, where he is currently an Associate Professor. His current research interests include electrical machine design, modelling, and control. He has participated in various research projects in the fields of wind energy systems, lift drives, and railway traction.

Javier Poza was born in Bergara, Spain, in June 1975. He received the B.S. degree in electrical engineering from the University of Mondragón, Mondragón, Spain, in 1999 and the Ph.D. degree in electrical engineering from the Institut National Polytechnique de Grenoble, Grenoble, France. Since 2002, he has been with the Department of Electronics, Faculty of Engineering, University of Mondragón, where he is currently an Associate Professor. His current research interests include electrical machine design, modelling, and control. He has participated in various research projects in the fields of wind energy systems, lift drives, and railway traction.

Gaizka Ugalde received the B.S. and the Ph.D. degrees in electrical engineering from the University of Mondragón, Mondragón, Spain, in 2006 and 2009, respectively. Since 2009, he has been with the Department of Electronics, Faculty of Engineering, University of Mondragón, where he is currently an Associate Professor. His current research interests include permanent-magnet machine design, modelling, and control. He has participated in various research projects in the fields of lift drives and railway traction.

Ana Julia Escalada was born in Pamplona, Spain, in April 1977. She received the B.S. degree in electronic engineering from the University of the Basque Country, Bilbao, Spain, in 2001, the B.S. degree in physics from the University of Cantabria, Santander, Spain, in 2003, and the Ph.D. degree in automatic and industrial electronic engineering from the University of Mondragón, Mondragón, Spain, in 2007, in conjunction with the Power Electronics Department, Ikerlan Technological Research Center.

She is currently with the Electrical Drives Department, ORONA Elevator Innovation Centre, Hernani, Spain. Her interests are drives and electrical machines for lifts.